European Journal of Pharmaceutics and Biopharmaceutics 75 (2010) 334–340

Contents lists available at ScienceDirect

European Journal of Pharmaceutics and Biopharmaceutics

journal homepage: www.elsevier.com/locate/ejpb

Research paper

Enhanced cytotoxicity and activation of ROS-dependent c-Jun NH_2-terminal kinase and caspase-3 by low doses of tetrandrine-loaded nanoparticles in Lovo cells – A possible Trojan strategy against cancer

Xiaolin Li [a,e,1], Donghui Zhen [b,1], Xiaowei Lu [a,1], Hua'e Xu [c], Yun Shao [a], Qiping Xue [a], Yong Hu [d], Baorui Liu [e,*], Weihao Sun [a,**]

[a] Department of Geriartrics, The First Affiliated Hospital of Nanjing Medical University, Nanjing, PR China
[b] Department of Nephrology, Huai'an Second Hospital Affiliated to Xuzhou Medical College, Huai'an, PR China
[c] Department of Pharmacy, The First Affiliated Hospital of Nanjing Medical University, Nanjing, PR China
[d] Laboratory of Mesoscopic Chemistry and Department of Polymer Science and Engineering, Nanjing University, Nanjing, PR China
[e] The Comprehensive Cancer Center of Drum Tower Hospital Affiliated to Medical School of Nanjing University & Clinical Cancer Institute of Nanjing University, Nanjing, PR China

ARTICLE INFO

Article history:
Received 12 November 2009
27 April 2010
Accepted in revised form 28 April 2010
Available online 11 May 2010

Keywords:
Tetrandrine
Nanoparticle
Anti-tumor
Reactive oxygen species (ROS)
c-Jun NH_2-terminal kinase
Caspase-3

ABSTRACT

Tetrandrine (Tet), a bis-benzylisoquinoline alkaloid, has recently been reported as a novel anti-cancer agent in vitro and in vivo by inducing apoptosis with the formation of reactive oxygen species (ROS) and the activation of ROS-dependent c-Jun NH_2-terminal kinase (JNK) and caspase-3. However, application of Tet is limited for its insolubility. Accumulated evidences raise the possibility of developing nanoscale delivery systems of Trojan strategy with improved solubility, stability and cytotoxicity of lipophilic Tet. Here, we reported first a simple way to produce Tet-loaded nanoparticles based on amphiphilic block copolymer. The controlled release pattern of Tet-loaded nanoparticles (Tet-np) was characterized by in vitro release experiments. Cytotoxicity tests proved anti-tumor effect of Tet-np against Lovo cells. Moreover, doses of Tet-np during lower concentrations (1–8 μg/ml) led to more cell inhibition than equivalent doses of free Tet did (1–8 μg/ml). It was further presented that the higher uptake efficiency, more reactive oxygen species (ROS) generation, and the stronger activation of ROS-dependent c-Jun NH_2-terminal kinase (JNK) and caspase-3 were induced by the equivalent dose of Tet delivered by nanoparticles. Although the present results suggested that Tet-np could be a potential useful chemotherapeutic tool, intensive researches are still warranted.

1. Introduction

Many chemotherapeutics induce the death of cancer cells through elevating the level of intracellular reactive oxygen species (ROS) [1]. Overproduced ROS aim at various targets including proteins, lipids and nucleic acid so as to injury cells, which also stimulate proapoptotic signal molecules such as c-Jun-NH_2-kinase [2], activate p38 and p53 protein pathway [3], or trigger the mitochondrial apoptotic cascade [4].

Latest studies revealed that tetrandrine (Tet), a bis-benzylisoquinoline alkaloid, isolated from the root of *Stephania tetrandra*, had anti-tumor capacity both in cultured tumor cells and animal models [4–11]. Tet can effectively induce oxidative stress leading to elevated intracellular ROS [7–9]. Then ROS-dependent c-Jun N-terminal protein kinase (JNK) and caspase-3 are sequentially activated by elevated ROS [1,4,8,9], which results in the apoptosis of tumor cells. Applications of this potential anti-cancer agent are, however, restricted by the low bioavailability caused by its physical properties [4–12].

Recent progress in drug delivery has focused on improving drug delivery for malignant disease by nanomedicine and polymer techniques. Among them, amphiphilic block copolymer-based polymeric micelles can self-assemble into nanoparticles with hydrophilic outer shells and hydrophobic inner cores [13]. These nanoparticles capture hydrophobic drug in the cores and disperse easily in solution with the protection of hydrophilic shells, which are easy to be internalized by cells [13]. Drug-loaded polymeric nanoparticles were proved to be a valuable controlled delivery system for passive-targeting administration of therapeutics by virtue of endocytosis in vitro and the Enhanced Permeability and Retention (EPR) effect in vivo [13,14].

* Corresponding author. The Comprehensive Cancer Center of Drum Tower Hospital Affiliated to Medical School of Nanjing University & Clinical Cancer Institute of Nanjing University, Nanjing 210008, PR China. Tel./fax: +86 25 83107081.
** Corresponding author. Department of Geriartrics, The First Affiliated Hospital of Nanjing Medical University, Nanjing 210029, PR China. Tel./fax: +86 25 68135151.
E-mail addresses: baoruiliu@nju.edu.cn (B. Liu), weihaosun@hotmail.com (W. Sun).
[1] These authors contributed equally to this article.

0939-6411/$ - see front matter © 2010 Elsevier B.V. All rights reserved.
doi:10.1016/j.ejpb.2010.04.016

It has also been used to enhance gene or protein delivery efficiency [13].

The lipophilicity of Tet raises the possibility of developing Tet-loaded biodegradable polymeric micelles delivery systems. Whether or not the Trojan strategy of nanoparticle-based Tet delivery can effectively induce intracellular ROS accumulation and stimulate activation of ROS-dependent JNK and caspase-3 is unclear.

Previously reported amphiphilic block copolymer-based nanoparticles, composed of polycaprolactone (PCL) and polyethylene glycol (PEG) [13], were chosen to develop a controlled drug delivery system containing Tet. The physical characterizations and the delivery efficiency of nanoparticles to Lovo cells based on coumarin-6 loaded nanoparticles were evaluated. We further studied the discrepancy of in vitro cytotoxicity, intracellular ROS induction and the activation of ROS-dependent JNK and caspase-3 between Tet-np and free Tet. According to the results, we propose the hypothesis that delivery of Tet via nanoparticles might effectively induce ROS generation and therefore activate proapoptotic signal molecules in cancer cells.

2. Materials and methods

2.1. Materials

Tetrandrine was kindly provided by Zhejiang Haizheng Pharmceutical Co., Ltd. According to our previous work [15,16], PCL20k–PEG4k nanoparticles were applied in the following procedure for their higher drug loading content and encapsulation efficiency. Human colon–rectum cancer cell line, Lovo cell line, was obtained from Shanghai Institute of Cell Biology (Shanghai, China). Cell culture material (RPMI Media 1640, fetal bovine serum, etc.) was from Invitrogen (Carlsbad, CA). 3-(4,5-dimethylthiazol-2-yl)-2,5-diphenyltetrazolium bromide (MTT) and 2,7-dichlorofluoroescin diacetate (H_2DCF-DA) were purchased from Sigma Chemical Co. (St. Louis, MO, USA). All other chemicals were of analytical grade and used without further purification.

2.2. Methods

2.2.1. Formulation of nanoparticles

Tet-loaded nanoparticles were prepared by a nanoprecipitation method as described previously with minor modification [15,16]. Briefly, 10-mg mPEG–PCL block copolymers and a predetermined amount of Tet were dissolved in 2 ml acetone. The obtained organic solution was added dropwise into 10 times volume of distilled water under gentle stirring at room temperature. The solution was dialyzed in a dialysis bag (molecular weight cut-off 12kd, Sigma–Aldrich Corp., St. Louis, MO, USA) to remove acetone thoroughly. The resulted bluish aqueous solution was filtered through a 0.22-μm filter membrane to remove non-incorporated drugs and copolymer aggregates. Coumarin-6-loaded nanoparticles were prepared by replacing Tet with coumarin-6. Drug-free nanoparticles were produced in a similar manner without adding drugs. Solutions of drug-loaded nanoparticles and empty nanoparticles were then lyophilized for further utilization.

2.2.2. Characterization of nanoparticles

Atomic force microscopy (AFM, SPI3800, Seiko Instruments, Japan) and transmission electron microscope (TEM, JEM-100S Japan) were used to visualize nanoparticles. Fourier transform infrared spectra (FTIR) were measured by a Perkin-Elmer Paragon 1000 Fourier transform spectrometer. In all cases, 64 scans at a resolution of 2 cm^{-1} were used to record the spectra. Mean diameter and size distribution were measured before lyophilization by photon correlation spectroscopy (DLS) using a Brookheaven BI-9000AT instrument (Brookheaven Instruments Corporation, NY, USA). Zeta potential was measured by the laser Doppler anemometry (Zeta Plus, Zeta Potential Analyzer, Brookhaven Instruments Corporation, NY, USA).

2.2.3. Drug loading content (DLS) and encapsulation efficiency (EE)

The concentration of Tet was assayed on a Shimadzu LC-10AD (Shimadzu, Japan) HPLC system equipped with a Shimadzu UV detector and an agilent C-18, 5 μm, 200 mm × 4.6 mm RP-HPLC analytical column. The mobile phase was consisting of methanol (spectral grade, Merck, Germany)/double-distilled water/ethylamine (90/10/0.05, v/v/v) pumped at a flow rate of 1.0 ml/min with determination wavelength of 282 nm. The concentration of Tet was determined based on the peak area at the retention time of 4.83 min by reference to a calibration curve. The following equations were applied to calculate the drug loading content (Eq. (1)) and encapsulation efficiency (Eq. (2)).

$$\text{Drug loading content } (\%) = \frac{\text{Weight of the drug in nanoparticles}}{\text{Weight of the nanoparticles}} \times 100\% \quad (1)$$

$$\text{Encapsulation efficiency } (\%) = \frac{\text{Weight of the drug in nanoparticles}}{\text{Weight of the feeding drugs}} \times 100\% \quad (2)$$

2.2.4. In vitro release of Tet-loaded nanoparticles

For in vitro release detection, 10 mg lyophilized Tet-loaded nanoparticles were suspended in 1 ml of 0.1 M phosphate-buffered saline (PBS, PH 7.4). The solution was then placed into a preswelled dialysis bag with a 12-kDa molecular weight cut-off (Sigma) and immersed into 20 ml 0.1 mol/l PBS, pH 7.4, at 37 °C with gentle agitation. One milliliter samples was withdrawn from the incubation medium and measured for Tet concentration as described earlier. After sampling, equal volume of fresh PBS was immediately added into the incubation medium. The concentration of Tet released from the nanoparticles was expressed as a percentage of the total Tet in the nanoparticles and plotted as a function of time.

2.2.5. Nanoparticle uptake by Lovo cells

Coumarin-6 was utilized as fluorescent marker to assess the efficiency of nanoparticle uptake by tumor cells. About 5×10^5 Lovo cells was seeded in 6-well plates with RPMI 1640 supplemented with 10% calf blood serum and allowed to adhere at 37 °C with 5% CO_2 for 24 h prior to the assay. The medium was then replaced with 10 ml fresh RPMI 1640 containing coumarin-6 loaded nanoparticles (indicated by dose of coumarin-6). After 4-h incubation, the cell monolayers were rinsed three times with PBS buffer to remove excess nanoparticles. The cells were viewed and imaged under a fluorescence microscope (Carl Zeiss LSM 410, Goettingen, Germany) using a FITC filter. By repeating the above-mentioned procedure while changing coumarin-6 concentration (5, 15, 30, 60 μg/ml), cells were incubated with different doses of coumarin-6-loaded nanoparticles, then collected for the quantitative analysis of nanoparticle uptake indicated by coumarin-6 content. The cell lysates were reconstituted in 500 μl methanol and sonicated for 30 s at 5w to extract the fluorescent dye from the nanoparticles. The samples were centrifuged at 12,000 rpm for 10 min at 4 °C, and 400 μl of the supernatants were collected for HPLC analysis. The concentration of coumarin-6 was assayed on a Shimadzu LC-10AD (Shimadzu, Japan) HPLC system equipped with a Shimadzu fluorescence detector (Model RF-10AXL; Ex(λ) 450 nm/Em(λ) 490 nm) and an agilent C-18, 5 μm, 200 mm × 4.6 mm RP-HPLC analytical column. The mobile phase was consisting of acetonitrile (spectral grade, Merck, Germany)/double-distilled water/1-

heptane sulfonic acid sodium salt (65/35/0.005, v/v/v) pumped at a flow rate of 1.0 ml/min. The concentration of coumarin-6 was determined based on the peak area by reference to a calibration curve. The efficiency of nanoparticle uptake was calculated from the amount of coumarin-6 detected in the cell and total added.

2.2.6. In vitro cytotoxicity studies

Cytotoxicity of Tet-loaded nanoparticles against Lovo cells was assessed by MTT assay [15]. Briefly, cells were seeded in 96-well plates with a density around 5000 cells/well and allowed to adhere for 24 h prior to the assay. Cells were exposed to a series of equivalent doses of free Tet or Tet-loaded nanoparticles (1, 2, 4, 8, 16, 32 μg/ml) at 37 °C. After 48 h of incubation, cold PBS (pH 7.4) was utilized to wash the cells carefully and then 50 μl of MTT indicator dye (5 mg/ml in PBS, pH 7.4) was added to each well and incubated for 2 h at 37 °C in the dark. The medium was withdrawn, and 200 μl acidified isopropanol (0.33 ml HCl in 100 ml isopropanol) was added to each well and agitated thoroughly to dissolve the formazan crystals. Absorption was measured at 550 nm in Microkinetics reader BT2000, and obtained values were expressed as a percentage of the controls.

2.2.7. Detection of intracellular ROS

H2DCF-DA was used to detect intracellular generation of ROS [1] by modification. Briefly, Lovo cells (2×10^5) were cultured with Tet or Tet-np at the equivalent Tet does of 4 μg/ml. After 48-h incubation, cells were incubated with 5 mM H2DCF-DA for 30 min. After washing three times with cold PBS, the intensity of fluorescence was determined by a fluorescence spectrophotometer under an emission wavelength at 535 nm (H2DCF-DA), while an excitation wavelength at 485 nm. The obtained values were expressed as folds of the controls. According to green fluorescence of DCF, typical images of intracellular ROS generation were obtained. The lighter the fluorescence, the greater the ROS generation.

Another indicator, dihydroethidium (DHE), was used to confirm the ROS generation in cells by different agents. The method was similar to that of H2DCF-DA except that the concentration of DHE was 10 μM. Emission wavelength was 610 nm and excitation wavelength was 535 nm.

2.2.8. Western blot analysis

Lovo cells (1×10^6) were cultured under the same conditions as in the in vitro ROS studies with Tet or Tet-np at the equivalent Tet

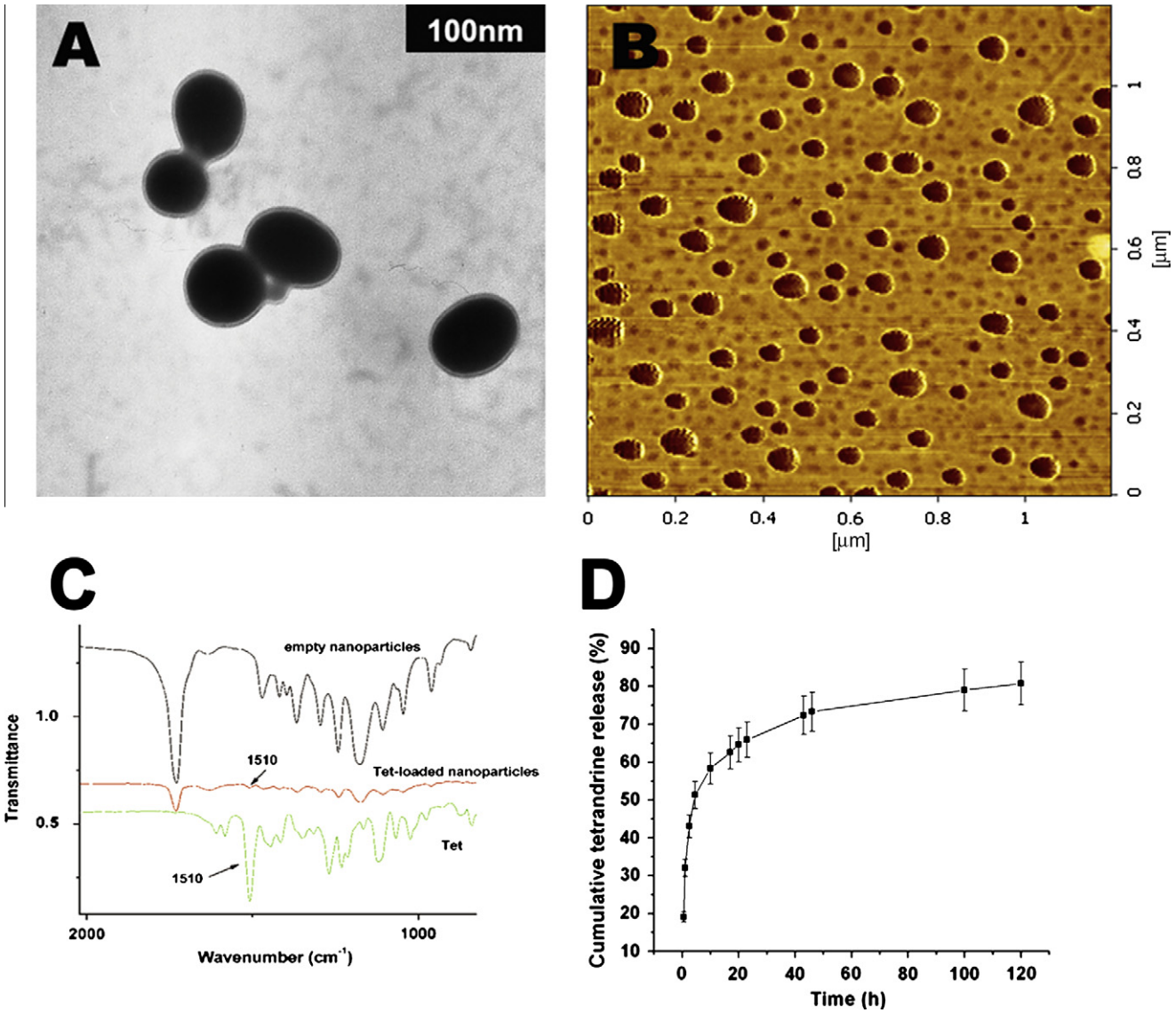

Fig. 1. Characterization of Tet-loaded nanoparticles. (A) TEM image of mPEG–PCL nanoparticles. (B) AFM image of mPEG–PCL nanoparticles. (C) The FTIR spectrums of free tetrandrine, empty nanoparticles and tetrandrine-loaded nanoparticles. (D) Cumulative in vitro release profile of tetrandrine from mPEG–PCL nanoparticles. (For interpretation of the references to colour in this figure legend, the reader is referred to the web version of this article.)

does of 4 μg/ml for 48 h. Protein levels of JNK1, p-JNK and procaspase-3 were analyzed by Western blot as described previously [17,18]. Briefly, cell lysates were prepared, electrotransferred, and then immunoblotted with anti-JNK1 (Santa Cruz Biotechnology), anti-phosphate-JNK (Sigma, USA) and anti-procaspase-3 (Santa Cruz Biotechnology). For phosphoprotein detection, cells were washed with ice-cold PBS containing 1 mM Na_3VO_4 and 1 mM NaF, and lysed in a buffer (20 mM Tris–Cl (pH 8.0), 137 mM NaCl, 10% glycerol, 1% TritonX-100, 1 mM Na_3VO_4, 1 mM NaF, 2 mM EDTA, 200 nM aprotinin, 20 mM leupeptin, 50 mM phenanthroline, 280 mM benzamidine-HCl) [17]. Detection was performed with Western blotting reagent ECL (Amersham), and chemiluminescence was exposed by the filters of Kodak X-Omat films. After normalizing the bands with the actin control, Image Pro Plus (Media Cybernetics, Silver Spring, MD, USA) was applied to perform the quantification analysis.

2.2.9. Caspase-3 activity assay

Lovo cells at a density of 1×10^6 cells/well were cultured under the same conditions as in the in vitro ROS studies and Western blot analysis. Determination of caspase-3 activity was performed by the caspase colorimetric protease assay kit (Keygen Biotech, Nanjing, China) by following the manufacturer's instruction. The optical density was measured at 405 nm. The obtained values were expressed as folds of controls.

2.2.10. Statistical analysis

Data were expressed as the mean ± SD of three independent experiments. Statistical analysis for the comparison of relative groups was based on student's *t*-test or one-way ANOVA analysis with SPSS 11.5 software (SPSS, USA). Significance was accepted at the 0.05 level of probability.

3. Results and discussion

3.1. Characterization of nanoparticles

The morphology of Tet-loaded nanoparticles was characterized by TEM and AFM. Both images showed the spherical shape of the polymeric nanoparticles with a smooth surface (Fig. 1A and B). DLS was utilized to determine the size and zeta potential of Tet-loaded nanoparticles. As shown in Table 1, the sizes are less than 100 nm. In accordance with previous reports, zeta potential test showed that Tet-loaded nanoparticles exhibit a negative zeta potential slightly below 0 mv, which indicated PEG outer shell is capable to screen the surface charge in certain degree [19,20]. The FTIR demonstrated that Tet is successfully incorporated into the nanoparticles [21,22]. From the spectrum of free Tet, some characteristic peaks could be obtained, such as 1510 cm^{-1}, which obviously localized in the spectrum of Tet-loaded nanoparticles (Fig. 1C). The hydrophobicity of Tet and the satisfied affinity between Tet and the hydrophobic core (PCL) [23,24] result in high loading efficiency. By varying the feeding ratio of copolymer and Tet, the highest drug loading content of Tet into mPEG4k–PCL20k nanoparticles was detected as 18.2 ± 2.1% and the encapsulation efficiency was more than 90% (Table 1).

Table 1
Mean particle size and drug load efficiency of two kinds of nanoparticles.

Nanoparticles	Particle size (nm)[a]	Polydispersity	Zeta potential (mV)	DLC (%)[b]	EE (%)[c]
mPEG4k–PCL20k	75.3 ± 4.9	0.14 ± 0.04	−6.1 ± 1.4	18.2 ± 2.1	92 ± 2.6

[a] The SD value was for the mean particle size obtained from the three measurements of a single batch.
[b] DLC = drug loading content.
[c] EE = encapsulation efficiency.

3.2. In vitro release of Tet-loaded nanoparticles

Fig. 1D shows the sustained release profile of Tet-loaded nanoparticles. An initial burst of more than 50% release in 5 h indicated that like other core–shell delivery systems, the affiliation of certain drugs to the surface of the nanoparticles is unavoidable. In the following period, release of Tet was observed in a sustained manner from nanoparticles. Finally, 5 days incubation with PBS caused a total 80% higher release. These data indicated that incorporated Tet could be released from the core–shell structure of polymeric nanoparticles, and the Tet-loaded nanoparticles might be a potential controlled release system for cancer therapy.

3.3. Uptake of nanoparticles by Lovo cells

Fig. 2A and B revealed the cellular uptake of coumarin-6-loaded nanoparticles. It was obvious that 4-h incubation was sufficient for Lovo cells to uptake nanoparticles that were localized in the cyto-

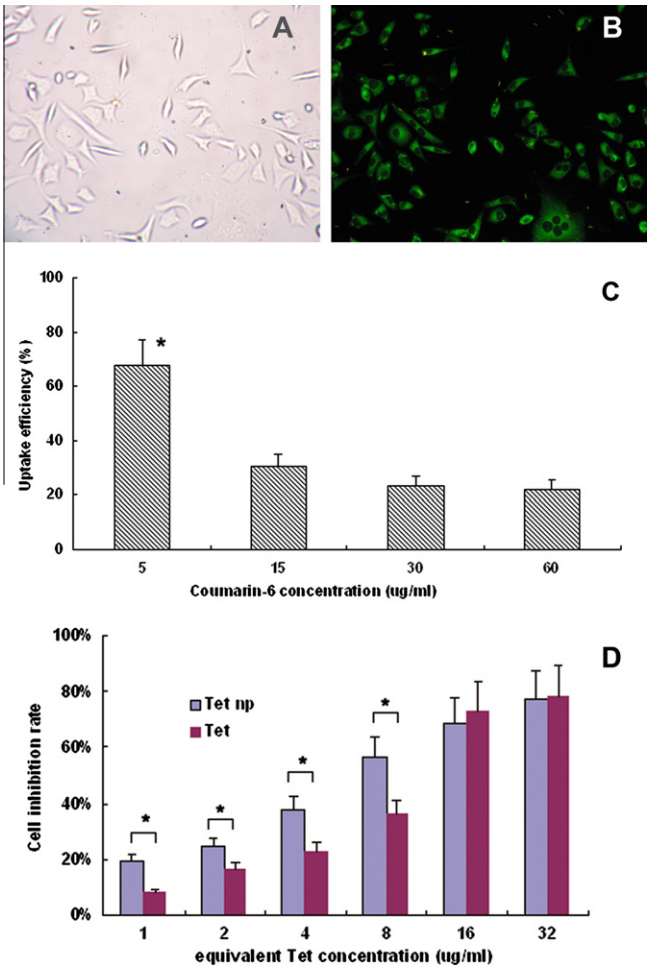

Fig. 2. Uptake of coumarin-6-loaded nanoparticles by Lovo cells and Cctotoxicity of tetrandrine (Tet) and tetrandrine-loaded nanoparticles (Tet-np) against Lovo cells. (A and B) Microscopic images of Lovo cells incubated with coumarin-6-loaded nanoparticles (A: bright field; B: fluorescent field. Magnification = 200×). (C) The efficiency of nanoparticle uptake by Lovo cells with different concentration of coumarin-6. (D) Cytotoxicity of tetrandrine (Tet) and tetrandrine-loaded nanoparticles (Tet-np) against Lovo cells after 48-h incubation. Statistics was performed by one-way ANOVA analysis (Fig. 2C) and student's *t*-test (Fig. 2D). * Means $p < 0.05$. Values represents Mean ± SD ($n = 3$). (For interpretation of the references to colour in this figure legend, the reader is referred to the web version of this article.)

plasm indicated by the fluorescence of coumarin-6 (Fig. 2B). Quantitative analysis showed that the uptake efficiency of nanoparticles by Lovo cells was significantly influenced by the concentration. Low concentration resulted in substantially high uptake efficiency, while increasing concentration led to reduced uptake efficiency (DF = 3, $F = 9.78$, $p < 0.05$, ANOVA) (Fig. 2C). Possible explanation would be that nanoparticles were uptaken by cells through endocytosis. When the concentration of nanoparticles is beyond saturable capacity of cell endocytosis, the uptake efficiency will not increase with the concentration elevating [25].

3.4. In vitro cytotoxicity of nanoparticles to Lovo cells

The results of in vitro cytotoxicity tests were showed in Fig. 2D. Blank nanoparticles were nearly non-toxic to cells with the inhibition rate less than 8% even at a high nanoparticle concentration of 500 μg/ml (data not shown). Both Tet and Tet-loaded nanoparticles displayed similar dose-dependent cell inhibition effects after 48 h. Noticeably, Tet-loaded nanoparticles showed significantly stronger cytotoxicity than equivalent dose of Tet when the doses were below 8 μg/ml ($p < 0.05$, *t-test*). For instance, 4 μg/ml Tet-loaded nanoparticles resulted in near 35% cell inhibition, while the same dose of Tet caused about 20% cell death. However, at equivalent doses over 8 μg/ml, Tet-loaded nanoparticles induced similar cell inhibition with Tet. Previous reports supported the current findings not only by investigating the cellular uptake efficiency of fluorescence but also by determining the cytotoxicity of drug-loaded nanoparticles at low concentrations [25,26]. Based on the above results, low Tet dose of 4 μg/ml was chosen to further elucidate the superiority of Tet-np over free Tet at low concentration through detection of ROS level, Western blot analysis of p-JNK and JNK and in vitro assay of caspase-3 activation.

3.5. Detection of ROS level

Recent studies have demonstrated that some anti-tumor chemopreventive drugs induce tumor cell death via ROS generation. Overproduction of intracellular ROS is one of the mechanisms involved in Tet-mediated apoptosis of cancer cells [2,4]. In our experiment, ROS were detected by H2DCF-DA in cells treated with Tet and Tet-np. As shown in Fig. 3A, Lovo cells as control and treated with empty nanoparticles (E-np) had weak background fluorescence resulting from cell metabolism [1], while treatment with either Tet or Tet-np greatly increased the population of Lovo cells with bright DCF fluorescence, which indicated the increase in intracellular ROS. Quantitative analysis of intracellular ROS level demonstrated that there was no significant difference between control and treatment with E-np, but incubation with Tet or Tet-np elevated intracellular ROS level to 3.4- or 5.1-folds of control (DF = 3, $F = 6.78$, $p < 0.05$, ANOVA), respectively (Fig. A1–E1). Moreover, Tet-np (4 μg/ml) induced higher intracellular ROS accumulation than equivalent dose of free Tet ($p < 0.05$, ANOVA). The role of

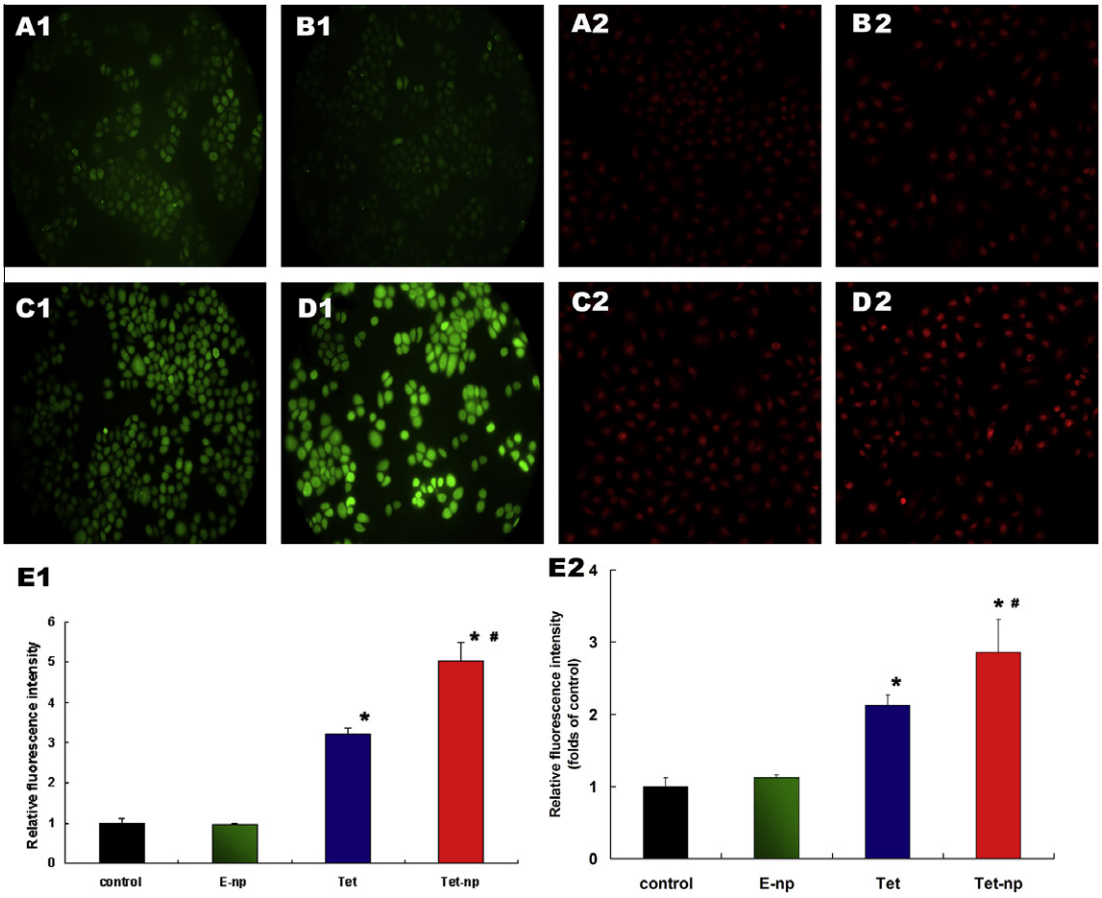

Fig. 3. Detection of intracellular ROS by DCFH and DHE. Fluorescence images of Lovo cells treated with different agents. The brighter the fluorescence, the greater the ROS production. A1–D1: DCF fluorescence images of Lovo cells treated with different agents. A2–D3: DHE fluorescence images of Lovo cells treated with different agents. A1 and A2: Control containing vehicle. B1 and B2: Empty nanoparticles (E-np). C1 and C2: Tet (4 μg/ml). D1 and D2: Tet-loaded nanoparticles (Tet-np, at an equivalent dose of 4 μg/ml). E: Intracellular fluorescence intensity (E1: DCF fluorescence; E2: DHE fluorescence) of Lovo cells treated with above agents. Values represents Mean ± SD. * Represents $p < 0.05$ vs. control (one-way ANOVA). # Represents $p < 0.05$ vs. Tet (one-way ANOVA) ($n = 3$). (For interpretation of the references to colour in this figure legend, the reader is referred to the web version of this article.)

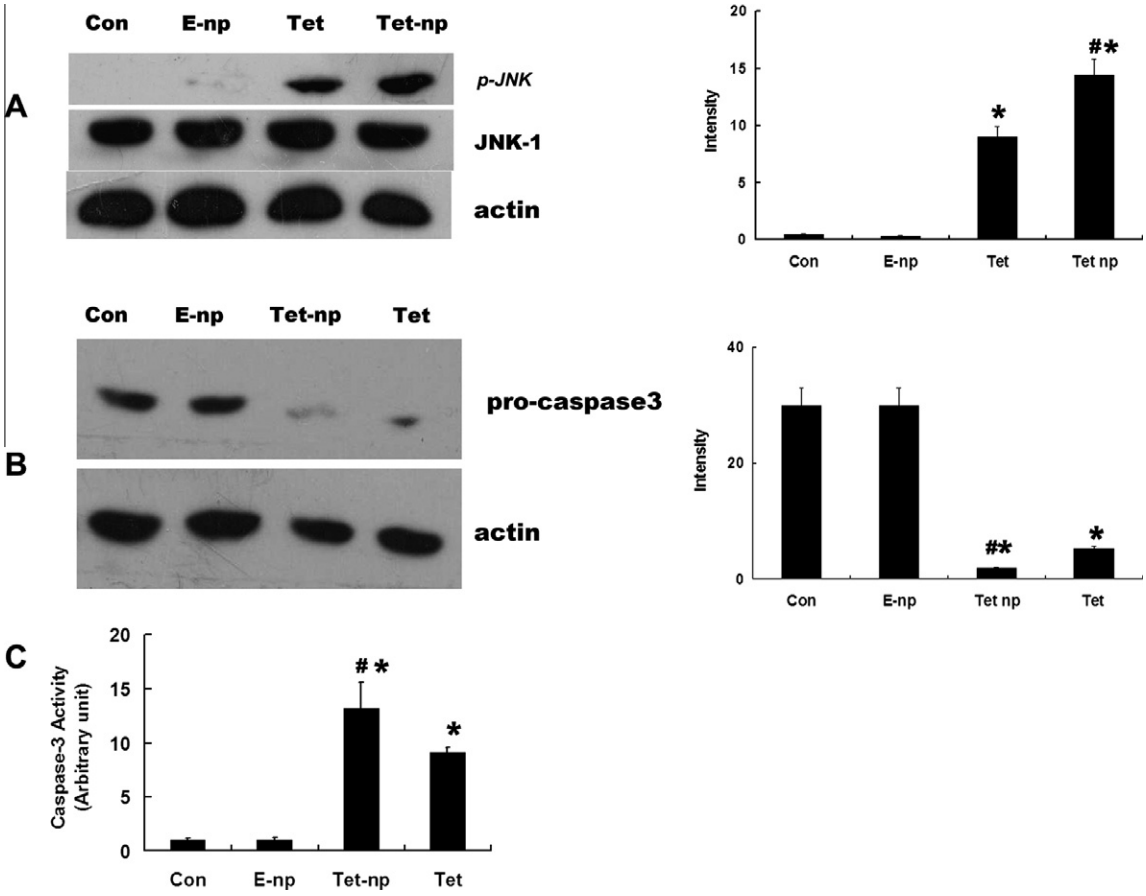

Fig. 4. Effects of tetrandrine (Tet) and tetrandrine-loaded nanoparticles (Tet-np) on activation of JNK and caspase-3 in Lovo cells (Lovo cells were treated with same agents as those defined in ROS detection). (A) Western blot analysis of p-JNK and JNK. Left: gel image; right: bargraph representing the semi-quantification of gel image (p-JNK/JNK) normalizing the band with the actin control. (B) Western blot analysis of procaspase-3. Left: gel image; Right: bargraph representing the semi-quantification of gel image (procaspase-3) normalizing the band with the actin control. (C) Activation analysis of caspase-3. Values represents Mean ± SD. * Represents $p < 0.05$ vs. control (one-way ANOVA). # Represents $p < 0.05$ vs. Tet (one-way ANOVA) ($n = 3$).

ROS acted in the tetrandrine-induced apoptosis complied with the determination of the viability of Lovo cells treated with Tet or Tet-np (4 μg/ml) for 48 h.

To confirm the ROS variation in Lovo cells exposed to different agents, we use DHE as the indicator for the generation of ROS. The results are similar to the outcome observed from H2DCF-DA. As shown in Fig. 3A2–E2, Tet-np (4 μg/ml) induced higher intracellular ROS accumulation than equivalent dose of free Tet (DF = 3, $F = 5.36$, $p < 0.05$, ANOVA).

3.6. Activation of JNK

ROS are known to activate JNK or p38 MAPK, and activities of these kinases are linked to apoptosis [1–4]. Western blot analysis showed that total JNK protein did not change after treatment with Tet/Tet-np while phosphate-JNK elevated, which indicated that Tet-induced activation of pre-existing JNK. High intracellular level of ROS induced by Tet/Tet-np companied by JNK activation in Tet-inducing Lovo cell inhibition indicated that Tet-induced ROS accumulation could activate JNK and might promote apoptosis. By normalizing the band with the actin control, the ratio of p-JNK to JNK (p-JNK/JNK) indicated that Tet-loaded nanoparticles at lower concentration (4ug/ml) led to more JNK activation compared to equivalent dose of free Tet (DF = 3, $F = 6.35$, $p < 0.05$, ANOVA) (Fig. 4A).

3.7. Activation of caspase-3

Intracellular ROS accumulation can directly trigger the apoptotic cascade [4], and the activation of caspases is important for tetrandrine-induced apoptosis in various tumor cells [4,27]. Tet-induced apoptosis is associated with intracellular ROS accumulation, which mediates the activation of both the upstream caspase-9 and the downstream effector caspase-3 [27]. Here, we measured the activity of downstream effector caspase-3 in Lovo cells treated with Tet or Tet-np. Western blot analysis showed that 48-h incubation with either Tet or Tet-np (4 μg/ml) resulted in a decrease in the inactive proform of caspase-3 (procaspase-3) in Lovo cells. Quantification analysis revealed that Tet-loaded nanoparticles at lower concentration (4 μg/ml) led to more decrease in the inactive proform than equivalent dose of free Tet did (DF = 3, $F = 6.94$, $p < 0.05$, ANOVA) (Fig. 4B). To quantify the activity of caspase-3, we performed an in vitro assay by caspase colorimetric protease assay kit as shown in Fig. 4C. When compared to control, treatment with Tet/Tet-np (4 μg/ml) for 48 h significantly activated caspase-3 with about 8-fold increase and 13-fold increase in caspase-3 activity, respectively (DF = 3, $F = 5.69$, $p < 0.05$, ANOVA).

Obviously, Tet-np statistically surpassed Tet in activating ROS-dependent JNK and caspase-3. Further studies are needed to clarify the relation between JNK pathway and caspase-3 demonstrated in Tet-inducing apoptosis.

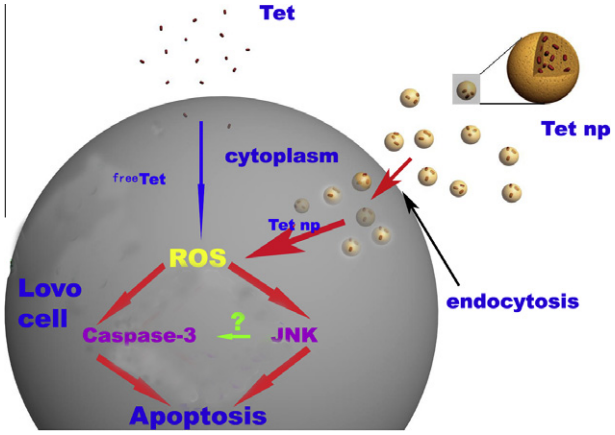

Fig. 5. The Trojan strategy of nanoparticle-based Tet delivery can effectively lead to higher cell death. Higher uptake efficiency underlied by endocytosis of low doses of Tet-np than equivalent doses of free Tet probably counted for the discrepancy of intracellular Tet accumulation, ROS levels and sequential activation of ROS-dependent JNK and caspase-3, all of which would mediate the superior cytotoxicity of Tet-np over free Tet. (For interpretation of the references to colour in this figure legend, the reader is referred to the web version of this article.)

4. Conclusion

The current study reported a simple way to efficiently produce controlled releasing Tet-loaded nanoparticles by amphilic mPEG-PCL block copolymers. The availability of Trojan strategy for Tet delivery was proved in Lovo cells. Higher uptake efficiency of low doses of Tet-np than equivalent doses of free Tet mediated by endocytosis, which leading to more intracellular Tet accumulation, inducing higher ROS level and stimulating stronger activation of ROS-dependent JNK and caspase-3, can underlie the result that Tet-loaded nanoparticles at lower doses led to higher cell death than equivalent doses of free Tet in Lovo cells (Fig. 5). The combination of Tet- and nanoparticle-based delivery system may generate promising outcomes in cancer therapy. It is undoubtedly, however, that the Trojan strategy of developing Tet-containing nanoscale drug delivery system warrants more intensive research.

Acknowledgment

This work was supported by the National Natural Science Foundation of China (No. 30872471), Jiangsu Province Key Medical Cent Foundation and Scientific and Technological Innovation Plan Fund of Postgraduate from Jiangsu Province (JX22013081).

Appendix A. Supplementary material

Supplementary data associated with this article can be found, in the online version, at doi:10.1016/j.ejpb.2010.04.016.

References

[1] Laurent, C. Nicco, C. Chereau, C. Goulvestre, J. Alexandre, A. Alves, E. Levy, F. Goldwasser, Y. Panis, O. Soubrane, B. Weill, F. Batteux, Controlling tumor growth by modulating endogenous production of reactive oxygen species, Cancer Res. 65 (2005) 948–956.
[2] M. Benhar, I. Dalyot, D. Engelberg, A. Levitzki, Enhanced ROS production in oncogenically transformed cells potentiates c-Jun N-terminal kinase and p38 mitogen-activated protein kinase activation and sensitization to genotoxic stress, Mol. Cell Biol. 21 (2001) 6913–6926.
[3] K. Tobiume, A. Matsuzawa, T. Takahashi, ASK1 is required for sustained activations of JNK/p38 MAP kinases and apoptosis, EMBO Rep. 2 (2001) 222–228.
[4] S.H. Oh, B.H. Lee, Induction of apoptosis in human hepatoblastoma cells by tetrandrine via caspase-dependent Bid cleavage and cytochrome *c* release, Biochem. Pharmacol. 66 (2003) 725–731.
[5] P.L. Kuo, C.C. Lin, Tetrandrine-induced cell cycle arrest and apoptosis in HepG2 cells, Life Sci. 73 (2003) 243–252.
[6] J.H. Lee, G.H. Kang, K.C. Kim, K.M. Kim, D.I. Park, B.T. Choi, H.S. Kang, Y.T. Lee, Y.H. Choi, Tetrandrine-induced cell cycle arrest and apoptosis in A549 human lung carcinoma cells, Int. J. Oncol. 21 (2002) 1239–1244.
[7] Y.J. Chen, Potential role of tetrandrine in cancer therapy, Acta Pharmacol. Sin. 23 (2002) 1102–1106.
[8] Q. Jin, C. Kang, Y. Soh, N.W. Sohn, J. Lee, Y.H. Cho, H.H. Baik, I. Kang, Tetrandrine cytotoxicity and its dual effect on oxidative stress-induced apoptosis through modulating cellular redox states in Neuro 2a mouse neuroblastoma cells, Life Sci. 71 (2002) 2053–2066.
[9] B.C. Janga, K.J. Lima, J.H. Paikb, J.W. Choc, W.K. Baeka, Tetrandrine-induced apoptosis is mediated by activation of caspases and PKC-d in U937 cells, Biochem. Pharmacol. 67 (2004) 1819–1829.
[10] C.L. Dai, H.Y. Xiong, L.F. Tang, X. Zhang, Y.J. Liang, M.S. Zeng, L.M. Chen, X.H. Wang, L.W. Fu, Tetrandrine achieved plasma concentrations capable of reversing MDR in vitro and had no apparent effect on doxorubicin pharmacokinetics in mice, Cancer Chemother. Pharmacol. 60 (5) (2007) 741–750.
[11] J.M. Wu, Y. Chen, J.C. Chen, T.Y. Lin, S.H. Tseng, Tetrandrine induces apoptosis and growth suppression of colon cancer cells in mice, Cancer Lett. 287 (2) (2010) 187–195.
[12] H.S. Cho, S.H. Chang, Y.S. Chung, J.Y. Shin, S.J. Park, E.S. Lee, S.K. Hwang, J.T. Kwon, A.M. Tehrani, M. Woo, M.S. Noh, H. Hanifah, H. Jin, C.X. Xu, M.H. Cho, Synergistic effect of ERK inhibition on tetrandrine-induced apoptosis in A549 human lung carcinoma cells, J. Vet. Sci. 10 (1) (2009) 23–28.
[13] Y. Hu, J. Xie, Y.W. Tong, C.H. Wang, Effect of PEG conformation and particle size on the cellular uptake efficiency of nanoparticles with the HepG2 cells, J. Control. Release 118 (2007) 7–17.
[14] H. Maeda, J. Wu, T. Sawa, Y. Matsumura, K. Hori, Tumor vascular permeability and the EPR effect in macromolecular therapeutics: a review, J. Control. Release 65 (2000) 271–284.
[15] X.L. Li, R.T. Li, X.P. Qian, Y.T. Ding, Y.X. Tu, R. Guo, Y. Hu, X.Q. Jiang, W.H. Guo, B.R. Liu, Superior antitumor efficiency of cisplatin-loaded nanoparticles by intratumoral delivery with decreased tumor metabolism rate, Eur. J. Pharm. Biopharm. 70 (2008) 726–734.
[16] X.W. Lu, C.B. Ji, H.E. Xu, X.L. Li, H.X. Ding, M. Y, Z.S. Zhu, D. Ding, X.Q. Jiang, X.S. Ding, X.R. Guo, Resveratrol-loaded polymeric micelles protect cells from Aβ-induced oxidative stress, Int. J. Pharm. 375 (2009) 89–96.
[17] F.M. Tang, K. John, Y.T. Lin, S.T. Liao, A.N. Lin, J.L. Xiang, Androgen via p21 inhibits TNF-α-induced JNK activation and apoptosis, doi: 10.1074/jbc.M109.042994.
[18] K.S. Lee, I.A. Kanae, K. Iijima, W.J. Lee, J. H. Lee, K. Yu, D.S. Lee, JNK/FOXO-mediated Neuronal Expression of Fly Homologue of Peroxiredoxin II Reduces Oxidative Stress and Extends Lifespan, doi: 10.1074/jbc.M109.028027.
[19] L. Zhang, M. Yang, Q. Wang, Y. Li, R. Guo, X. Jiang, C. Yang, B. Liu, 10-Hydroxycamptothecin loaded nanoparticles: preparation and antitumor activity in mice, J. Control. Release 119 (2007) 153–162.
[20] L. Zhang, Y. Hu, X. Jiang, C. Yang, W. Lu, Y. Yang, Camptothecin derivative-loaded poly(caprolactone-co-lactide)-b–PEG–b-poly(caprolactone-co-lactide) nano-particles and their biodistribution in mice, J. Control. Release 96 (2004) 135–148.
[21] R. Gref, Y. Minamitake, M.T. Peracchia, V. Trubetskoy, V. Torchilin, R. Langer, Biodegradable long-circulating polymeric nanospheres, Science 263 (1994) 1600–1603.
[22] Allen, D. Maysinger, A. Eisenberg, Nano-engineering block copolymer aggregates for drug delivery, Colloids Surf. B. Biointerfaces 16 (1999) 3–27.
[23] Y. Li, L. Dong, A. Jia, X. Chang, H. Xue, Preparation and characterization of solid lipid nanoparticles loaded traditional Chinese medicine, Int. J. Biol. Macromol. 38 (2006) 296–299.
[24] M. Wang, W. Chen, H. Zhang, X. Li, Y. Zhang, K. Yao, F. Yao, Synthesis and characterization of PLLA–PLCA–PEG multiblock copolymers and their applications in modifying PLLA porous scaffolds, Eur. Polym. J. 43 (2007) 4683–4694.
[25] J. Davda, V. Labhasetwar, Characterization of nanoparticle uptake by endothelial cells, Int. J. Pharm. 233 (2002) 51–59.
[26] L.E. van Vlerken, Z. Duan, M.V. Seiden, M.M. Amiji, Modulation of intracellular ceramide using polymeric nanoparticles to overcome multidrug resistance in cancer, Cancer Res. 67 (2007) 4843–4850.
[27] P.C. Liao, C.H. Lieu, Cell cycle specific induction of apoptosis and necrosis by paclitaxel in the leukemic U937 cells, Life Sci. 76 (2005) 1623–1639.